

Time-magnitude correlations and time variation of the Gutenberg-Richter parameter in foreshock sequences

B. F. Apostol^{a*} and L. C. Cune^b

^aInstitute of Earth's Physics, ^b Institute of Physics and Nuclear Engineering
Magurele-Bucharest MG-6, POBox MG-35, Romania

*corresponding author, email: afelix@theory.nipne.ro

Abstract

The time dependence of the parameter of the Gutenberg-Richter (GR) magnitude distribution is computed for foreshock sequences of earthquakes, correlated with the main shock, by using the geometric-growth model of earthquake focus, the magnitude distribution of correlated earthquakes and the time-magnitude correlations, derived recently. It is shown that this parameter decreases in time in the foreshock sequence, from the background values down to the main shock. If correlations are present, this time dependence and the time-magnitude correlations provide a tool of monitoring the foreshock seismic activity. We discuss the relevance of such an analysis for the occurrence moment and the magnitude of a main shock. The discussion is applied to a few Vrancea main shocks and the precursory seismic activity of the l'Aquila earthquake. The limitations of such an analysis are discussed.

Key words: Gutenberg-Richter parameters; foreshock-aftershock sequences; correlated earthquakes; main shock; occurrence time

1 Introduction

Recently, Gulia and Wiemer (2019) suggested that the difference between the parameters (β) of the Gutenberg-Richter (GR) magnitude distribution of the aftershocks and the foreshocks can be used to estimate the occurrence of main shocks. Accompanying earthquake sequences have been analyzed by these authors for the Amatrice-Norcia earthquakes (24 August 2016, magnitude 6.2; 30 October 2016, magnitude 6.6) and the Kumamoto earthquakes (15 April 2016, magnitude 6.5 and 7.3). They found that the foreshock parameter β is lower than the background value (*e.g.*, by 10%), while the aftershock parameter is higher than the background value (*e.g.*, by 20%). A similar decrease in the parameter β has been reported for the foreshocks of the L'Aquila earthquake (6 April 2009, magnitude 6.3) by Gulia et al. (2016) and the Colfiorito, Umbria-Marche, earthquake (26 September 1997, magnitude 6) by De Santis et al. (2011). The analysis method employed by Gulia and Wiemer (2019) was recently questioned (Dascher-Cousineau et al. 2020, 2021; see also Gulia and Wiemer 2021). We put forward in this paper a method, based on a short-term analysis of the foreshocks, which may be relevant for estimating the occurrence time and the magnitude of the main shocks. The method is based on the correlations which may exist between foreshocks and the main shock.

The standard GR magnitude distribution is $P(M) = \beta e^{-\beta M}$ (moment magnitude M), where the parameter β varies in the range 1.15 to 3.45 (in decimal basis 0.5 to 1.5); the mean value $\beta = 2.3$ (in decimal basis $\beta = 1$) is usually accepted as a reference value (Stein and Wysession 2003; Udias 1999; Lay and Wallace 1995; Frohlich and Davis 1993). It has been shown (Apostol 2006) that $\beta = br$, where $b = 3.45$ (in decimal basis $3/2$) and r is a parameter characterizing the earthquake focus (see Appendix). The parameter r is a statistical parameter which reflects mainly the average number of dimensions of the focus. We expect the parameter r to vary between $r = 1/3$

and $r = 1$, with a mean value $r = 2/3$ ($\beta = 2.3$). The standard cumulative (excedence) GR distribution (earthquakes with magnitude greater than M) is $P_{ex}(M) = e^{-\beta M}$; it is used in its logarithmic form $\ln N(M) = \ln N(0) - \beta M$, where $N(M)$ is the number of earthquakes with magnitude greater than M .

According to these standard formulae, an increase in β indicates the occurrence of more small-magnitude earthquakes, which may appear in the aftershock region, while a decrease in β indicates, comparatively, more greater-magnitude earthquakes. A decrease in β in the foreshock region has been reported in many instances (see, *e.g.*, Gulia et al. 2016 and References therein), as well as an increase in the aftershock region (Gulia et al. 2018). In principle, a statistical description of the accompanying seismic activity implies a symmetric distribution in the foreshock-aftershock regions. However, after a main shock the condition of the seismic region may change appreciably, such that it is difficult to view the foreshocks and the aftershocks as members of the same statistical ensemble.

2 Correlations

Earthquakes which occur closely in time and space, like the earthquake sequence accompanying a main shock, may be correlated with the main shock (see Appendix). The magnitude distribution of the correlated earthquakes differs from the standard Gutenberg-Richter distribution discussed above (Apostol 2021). Judged by their time-dependence shape, the first part of the foreshock distribution indicated by Gulia and Wiemer (2019) may exhibit correlations, but correlations cannot be definitely assessed in the aftershocks distribution; a change in the seismicity conditions may be present for aftershocks. We discuss below a possible relevance of a correlated foreshock sequence for the occurrence of a main shock.

The earthquake correlations, as identified in Apostol (2021), are dynamical,

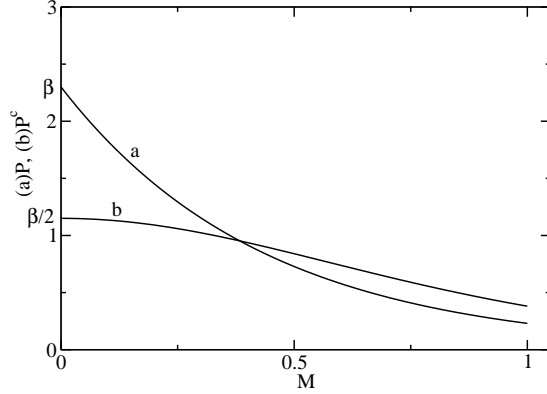


Figure 1: The standard GR distribution $P = \beta e^{-\beta M}$ (curve a) compared to the correlation-modified GR distribution P^c , Eq. (1) (curve b).

purely statistical and time-magnitude correlations. The dynamical correlations (called also "causal" correlations) imply a sharing of the accumulation time; they may also be viewed as temporal correlations. These correlations lead to modified statistical distributions, as the modified GR distribution given below. They may appear by a static or a dynamical stress, a change in the seismicity conditions of the focal region, a triggering mechanism, etc. Mathematical conditions (constraints) imposed on the statistical variables give rise to purely statistical correlations. Time-magnitude correlations, which are discussed in this paper, are particular dynamical correlations arising from the non-linearity of the law of energy accumulation in the focus. This law allows an energy sharing between two (or more) earthquakes, which makes an earthquake to depend on the other, *i.e.* it generates a correlation between these earthquakes (see Appendix).

The correlation-modified magnitude distribution (modified GR distribution, Apostol 2021) is

$$P^c(M) = \beta e^{-\beta M} \frac{2}{(1 + e^{-\beta M})^2} ; \quad (1)$$

without other specifications, this distribution includes the so-called dynamical correlations, which affect mainly the small-magnitude earthquakes. We

expect such correlations to be present in foreshock sequences. From Eq. (1) we get the correlation-modified cumulative distribution

$$P_{ex}^c(M) = e^{-\beta M} \frac{2}{1 + e^{-\beta M}} . \quad (2)$$

The logarithmic form of this distribution

$$\ln N^c(M) = \ln N(0) + \ln 2 - \ln (1 + e^{\beta M}) \quad (3)$$

should be compared to the standard logarithmic form

$$\ln N(M) = \ln N(0) - \beta M . \quad (4)$$

We can see that the modified GR distributions (Eqs. (1) and (2)) differ from the standard GR distributions, as shown in Figs. 1 and 2. It seems that such a qualitative difference has been found for southern California earthquakes recorded between 1945-1985 and 1986-1992 (Jones 1994). The difference arises mainly in the small-magnitude region $M \lesssim 1$, where the distributions are flattened. For instance, in this region the parameter β of the cumulative distribution tends to $\beta/2$, according to Eqs. (1) and (2) (see Appendix). This deviation, known as the roll-off effect (Bhattacharya et al. 2009; Pelletier 2000), is assigned usually to an insufficient determination of the small-magnitude data. We can see that it may be due to correlations, at least partially. For large magnitudes the logarithmic cumulative distribution is shifted upwards by $\ln 2$ (Eq. (3)), while its slope is very close to the slope of the standard cumulative GR distribution (β).

The correlation-modified cumulative distribution given by Eq. (2) can be used to identify a correlated sequence of foreshocks. We consider a seismic region with a background of earthquakes (regular earthquakes) extended over a long period of time T , interrupted from time to time by (rare) big seismic events. We may assume that some of these large earthquakes are

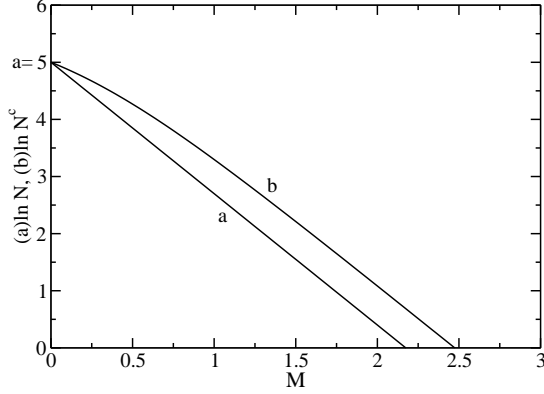


Figure 2: The standard cumulative GR distribution $\ln N = \ln N(0) - \beta M$ (curve a) compared to the correlation-modified cumulative GR distribution $\ln N^c$, Eq. (3) (curve b) for $\beta = 2.3$ and an arbitrary value $\ln N(0) = 5$.

main shocks in accompanying sequences of foreshocks (and aftershocks), correlated with the main shock. For moderate and large magnitudes we may fit the seismic activity by the standard cumulative GR distribution given by Eq. $\ln N(M) = \ln N(0) - \beta M$. Usually, such fits are done by using a small-magnitude cutoff, such that the slope of the distribution (β) is not affected by correlated small-magnitude earthquakes (difficulties in determining the β -parameter by finite sets of data and the related completeness magnitude are discussed recently by Marzocchi et al. 2020 and Lombardi 2021). A proper fitting of the full (modified) GR distribution given by Eq. (3) leads to very small differences in the parameter β . It is convenient to introduce the parameter $t_0 = T/N(0)$; its inverse is a seismicity rate. Due to the small-magnitude cutoff, this seismicity-rate parameter becomes a fitting parameter (Apostol 2021). The standard GR cumulative distribution reads

$$\ln [N(M)/T] = -\ln t_0 - \beta M . \quad (5)$$

By fitting this law to the empirical data we get the parameters β (and r) and t_0 . For instance, such a fit, done for a set of 3640 earthquakes with magnitude

$M \geq 3$ which occurred in Vrancea during 1981–2018, leads to $-\ln t_0 = 11.32$ (t_0 measured in years) and $\beta = 2.26$ ($r = 0.65$), with an estimated 15% error. We note that the value $\beta = 2.26$ is close to the reference value given above (2.3). (The data for Vrancea have been taken from the Romanian Earthquake Catalog 2018, <http://www.infp.ro/data/romplus.txt>. A completeness magnitude $M = 2.2$ to $M = 2.8$ is usually accepted (Enescu et al. 2008 and References therein); a more conservative figure would be $M = 3$. The magnitude average error is $\Delta M = 0.1$). A similar fit, with slightly modified parameters, is valid for 8455 Vrancea earthquakes with magnitude $M \geq 2$ (period 1980 – 2019). This way, we get the parameters of the background seismic activity for Vrancea (β, r, t_0).

3 Time-magnitude formula

Let us assume now that we are in the proximity of a main shock with magnitude M_0 , at time τ until its occurrence, and we monitor the sequence of correlated foreshocks. It was shown (Apostol 2021) that the magnitudes of the (correlated) foreshocks M ($< M_0$) are related to the time τ by

$$M \simeq \frac{1}{b} \ln(\tau/\tau_0) , \quad (6)$$

where

$$\tau_0 = r t_0 e^{-b(1-r)M_0} \quad (7)$$

is a cutoff time, which depends on the magnitude of the main shock, the seismicity-rate parameter t_0 and the parameter $r = \beta/b$ (see Appendix). The parameters t_0 and r are provided by the analysis of the background seismic activity. The small threshold time τ_0 corresponds to a very short quiescence time (Ogata and Tsuruoka 2016) before the occurrence of the main shock. In addition, the time τ should be cut off by an upper threshold, corresponding to the magnitude of the main shock ($\tau < \tau_0 e^{bM_0}$). We limit ourselves to small

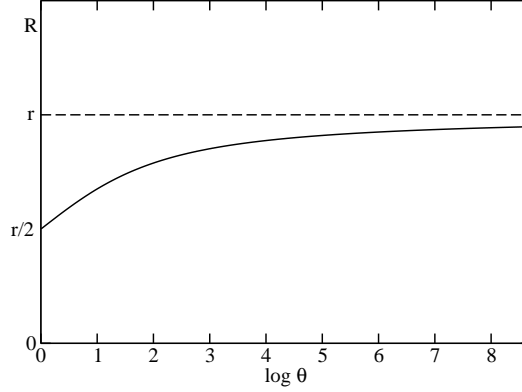


Figure 3: Function $R(\theta)$ vs $\log \theta$ for $r = 2/3$ (Eq. (9)).

and moderate magnitudes M in the accompanying seismic activity, such that the magnitude of the main shock may be viewed as being sufficiently large (in this respect, the so-called purely statistical correlations discussed by Apostol (2021), are not included). Eq. (6) is derived by analyzing the time-magnitude correlations predicted by the geometric-growth model of earthquake focus (Apostol 2006, see Appendix). According to this model the accumulation time of an earthquake with energy E is $t = t_0(E/E_0)^r = t_0 e^{\beta M}$, where E_0 is a cutoff energy. By means of this model, Bath's law is derived and the occurrence time of the Bath partner is calculated, as well as the cumulative magnitude distribution of the accompanying seismic activity.

The distribution given by Eq. (2) indicates a change in the parameter β of the standard GR distribution. We denote by B the modified parameter β ; it is given by

$$e^{-\beta M} \frac{2}{1 + e^{-\beta M}} = e^{-BM} , \quad (8)$$

where B is a function of M ($B(M)$). It is convenient to introduce the ratio $R = B/b$ (similar to $r = \beta/b$ given above), such that Eq. (8) becomes

$$R = \frac{1}{\ln \theta} \ln \left[\frac{1}{2} (1 + \theta^r) \right] , \quad (9)$$

where $\theta = \tau/\tau_0$ from Eq. (6). The parameter R varies from $R = r$ for large values of the variable θ to $R = r/2$ for $\theta \rightarrow 1$ ($\tau \rightarrow \tau_0$). The function $R(\theta)$ is plotted in Fig. 3 *vs* $\log \theta$ for $r = 2/3$. The decrease of the function $R(\theta)$ for $\theta \rightarrow 1$ indicates correlations.

According to Eq. (8), the modified GR parameter B is given approximately by

$$B(M) \simeq \beta - \frac{\ln 2}{M}, \quad (10)$$

or

$$R(\tau) \simeq r - \frac{\ln 2}{\ln(\tau/\tau_0)} \quad (11)$$

for a reasonable range of foreshock magnitudes $M > 1$. Eqs. (9)-(11) show the decrease of the GR parameter in a foreshock sequence. For instance, a 10% decrease is achieved for $M = 3$, or $\tau/\tau_0 \simeq 3.6 \times 10^4$ ($\beta = 2.3$, $r = 2/3$). It is worth noting that smaller magnitudes occur in the sequence of correlated foreshocks for shorter times, measured from the occurrence of the main shock (the nearer main shock, the smaller correlated foreshocks).

On the other hand, the time-magnitude correlations expressed by Eq. (6) lead to $\tau = \tau_0 e^{bM}$ for the accumulation time elapsed from the main shock to an aftershock. This relation shows a change in the seismicity conditions, where t_0 is replaced by τ_0 and β is replaced by b in the regular accumulation time $t = t_0 e^{\beta M}$. The magnitude distribution $(t_0/t^2) dt = \beta e^{-\beta M} dM$, which follows from this accumulation time (Apostol 2006, see Appendix), is changed in this case to $b e^{-bM} dM$, which indicates an increase in the GR parameter ($b = 3.45$) with respect to its background value β . Such a deviation holds up to a cutoff magnitude M_c where the two distributions become equal, such that we may estimate an average increase in the parameter β as $(b - \beta)/2\beta = 25\%$ for $\beta = 2.3$. The cutoff magnitude is given by $b e^{-bM_c} = \beta e^{-\beta M_c}$, whence $M_c = 0.36$ for $r = 2/3$, $b = 3.45$ ($\beta = 2.3$). Both these estimated deviations of the GR parameter for foreshocks and aftershocks are in quantitative agreement with data reported by Gulia et al. (2016, 2018) and Gulia and Wiemer (2019).

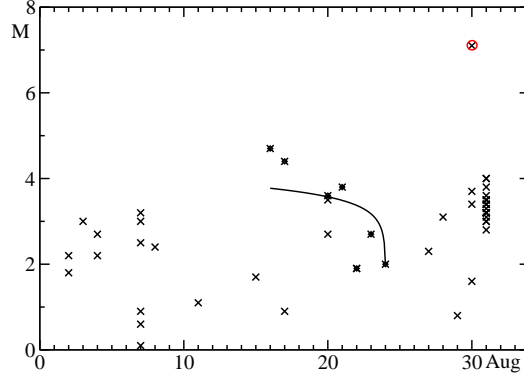


Figure 4: Vrancea seismic activity in the period 1 August - 31 August 1986 (Romanian Earthquake Catalog, 2018). The curve is the fit of Eq. (12) to data from 16 August to 24 August (fitting parameters $t_{ms} = 24$ August and $\tau_0 = 10^{-4.76}$ days; see text).

The logarithmic law expressed by Eq. (6) for the time-magnitude correlated foreshocks provides a means of estimating the occurrence time of the main shock. Indeed, if we update the slope B of the cumulative distribution $\ln[N(M)/N(0)] = -BM$ at various successive times t (Eq. (8)), and if this B fits Eq. (10), then we may say that we are in the presence of a correlated sequence of foreshocks which may announce a main shock at the moment $t_{ms} = t + \tau$. (In particular, the probability of occurrence of a main shock with magnitude M_0 increases in this case by a factor $\frac{\bar{B}}{\beta} e^{(\beta - \bar{B})M_0}$, where \bar{B} is the average value of the parameter B). For practical use it is more convenient to use directly Eq. (6), which leads to the time dependence

$$M(t) = \frac{1}{b} \ln \frac{t_{ms} - t}{\tau_0} \quad (12)$$

of the foreshock magnitudes, for $(1-r)t_{ms} < t < t_{ms} - \tau_0$ ($0 < M < M_0$). This formula provides an estimate of the occurrence moment of the main shock t_{ms} from the correlated-foreshock magnitudes $M(t)$ and the background seis-

micity parameter τ_0 ; the occurrence time is given by

$$t_{ms} = t + \tau_0 e^{bM(t)} . \quad (13)$$

It is worth noting that the time t_{ms} depends on the magnitude of the main shock, as expected (M_0 , which enters τ_0 , Eq. (7)). For instance, a magnitude M indicates a time $\tau = \tau_0 e^{bM}$ up to the main shock (Eq. (6)). Let us assume that we are interested in a main shock with magnitude $M_0 = 7$; then by using $t_0 = e^{-11.32}$ (years, for Vrancea) and $r = 2/3$ given above, we get $\tau_0 = \frac{2}{3} 10^{-8.42}$ (years); a foreshock with magnitude $M = 5$ would indicate that we are at $\tau = \frac{2}{3} 10^{-8.42} 10^{7.5} = 0.079$ years, *i.e.* $\simeq 29$ days, from that main shock. The time t_{ms} of the occurrence of the main shock is obtained from Eq. (12) as a fitting parameter of the correlated-foreshock magnitudes $M(t)$. In practice, it is also convenient to view τ_0 as a fitting parameter. Since, for moderate magnitudes, the variation of the parameter R is small (Eqs. (10) and (11)), we may use the background value for r in the expression of τ_0 (*e.g.*, $r = 2/3$), which leads to an estimate of the expected main-shock magnitude M_0 from the fitting parameter τ_0 . However, a reliable estimation of the time t_{ms} provided by Eq. (13) requires a very high slope of the decreasing magnitudes $M(t)$ in the neighbourhood of t_{ms} , which can only be attained by a special data set, including, ideally, many small-magnitude foreshocks whose magnitudes fall rapidly to zero.

4 Results

The application of Eqs. (12) and (13) to fitting the correlated foreshocks involves certain particularities. First, we should note that not all the precursory seismic events are foreshocks correlated with the main shock. Second, small clusters of precursory events may exist, which may include second-order (an even higher-order) correlated earthquakes, *i.e.* events which accompany

precursory events, according to the epidemic-type model (see, for instance, Ogata 1988, 1998, as well as Helmstetter and Sornette 2003 and Saichev and Sornette 2005). These secondary events have little relevance upon a forthcoming main shock, such that they may be left aside. We limit ourselves to the highest foreshocks occurring in short periods of time (though an average magnitude for each small cluster may also be used). Third, the relevant part of the logarithmic curve given by Eq. (12) (or the exponential in Eq. (13)) is its abrupt decrease in the immediate proximity of t_{ms} (of the order of days for Vrancea), such that we should limit ourselves to foreshocks which occur in the last few days. This limitation is related to the very small values of the parameter t_0 and the large magnitude M_0 , of interest for the main shock (small values of the parameter τ_0). In this regard, a reliable estimation of the parameters t_{ms} and τ_0 would be conditioned by a rich seismic activity in the immediate vicinity of the occurrence moment of a main shock (a very short-time prediction, *e.g.*, of the order of days). This is an ideal situation, which is not achieved in practice, since the number of small-magnitude foreshocks is small in the immediate vicinity of the main shock, precisely due to decrease of the parameter β (B , R). Therefore, such fits are necessarily of poor quality.

We give here a few examples of application of the fitting procedure described above.

Vrancea is the main seismic region of Romania. Reliable recordings of earthquakes started in Romania around 1980. Since then, three major earthquakes occurred in Vrancea: 30 August 1986, magnitude $M = 7.1$; 30 May 1990, magnitude $M = 6.9$; 31 May 1990, magnitude $M = 6.4$ (Romanian Earthquake Catalog 2018, <http://www.infp.ro/data/romplus.txt>). The 7.1-earthquake (depth $131km$) is shown in Fig. 4, together with all its precursory seismic events from 1 August to 31 August. All these earthquakes occurred in an area with dimensions $\simeq 100km \times 80km$ ($45^\circ - 46^\circ$ latitude, $26^\circ - 27^\circ$ longitude), at various depths in the range $30km - 170km$, except for the events

of 7-8 August and the 1.6-event of 30 August, whose depth was $5km - 20km$. The subset of earthquakes from 16 August to 24 August can be fitted by Eq. (12) with the fitting parameters $t_{ms} = 24$ August, $\tau_0 = 10^{-4.76}$ days and a large rms relative error 0.32. The maximum magnitude has been used for the earthquakes which occurred in the same day, because, very likely, those with smaller magnitude are secondary accompanying events of the greatest-magnitude shock. If we assume that this is a correlated-foreshock subset, it would indicate the occurrence of a main shock with magnitude 4.4 on 24 August. The main shock ($M = 7.1$) occurred on 30 August. The three earthquakes from 27 August to 29 August may belong to a subset prone to such an analysis, but it is too poor to be useful. A main shock with magnitude 7.1 ($\tau_0 = 10^{-6.06}$ days) and an average magnitude for the days with multiple events leads to a fit with a larger rms relative error 0.6. For the earthquake pair of 30-31 May 1990 (depth $87 - 91km$) we cannot identify a correlated subset of foreshocks, *i.e.* a sequence of precursory events with an average magnitude, or a maximum-magnitude envelope, decreasing monotonously in a reasonably short time range. Another particularity in this case, in comparison to the earthquake of 1986, is the quick succession (30-31 May) of two comparable earthquakes (magnitude 6.9-6.4).

In the set of precursory events of the l'Aquila earthquake, 6 April 2009 (magnitude 6.3, local magnitude 5.9) one can identify two magnitude-descending sequences, with earthquakes succeeding rapidly at intervals of hours. The first sequence occurred on 2 April, consisting of 7 earthquakes with local magnitudes from 2.1 to 1.0. The fitting of these data with Eq. (12) indicates a main shock approximately 5 hours before the earthquake with magnitude 3.0 of 3 April (with a large rms relative error 0.4). The second magnitude-descending sequence consists of 5 earthquakes with magnitudes from 1.9 to 1.1, which occurred on 6 April. The fit, with a similar large error, indicates the occurrence of a main shock at the time 01 : 35; the l'Aquila earthquake occurred at 01 : 32 (UTC; the last foreshock was recorded at 01 : 20). On the

other hand, a magnitude-descending sequence cannot be identified before the earthquake of 4 April, with local magnitude 3.9. The data used in this analysis are taken from the Bollettino Sismico Italiano, 2002-2012, in $\pm 25km$ an area around the epicentre of the l'Aquila earthquake (42.342° latitude, 13.380° longitude). The lack of the background seismicity parameters β and $-\ln t_0$ for the l'Aquila region prevents us from estimating the magnitude of the main shocks by this analysis. We note that the magnitude in the fitting Eq. (12) is the moment magnitude; the use of local magnitudes in this Eq. generates (small) errors.

We applied the same procedure to the Vrancea earthquake with magnitude 3.8 (local magnitude 4.1), viewed as a main shock, which occurred on 30 November 2021 (Apostol and Cune 2021). By making use of the foreshock sequence from 24 November to 27 November (5 earthquakes), we can predict a main shock on 28 November, with a large magnitude (6.9, with a small rms relative error). On 28 November an earthquake with magnitude 3.1 was recorded in this area. By extending the sequence until 29 November (7 earthquakes), a main shock with magnitude 4.5 was forecasted on 1 December (all the data are taken from Romanian Earthquake Catalog 2018, <http://www.infp.ro/data/romplus.txt>). All these earthquakes occurred within $45^\circ - 46^\circ$ latitude, $26^\circ - 27^\circ$ longitude, at depths in the range $90km - 180km$.

5 Conclusions

In conclusion, the GR distributions modified by correlations in the foreshock region and the time dependence of the foreshock magnitudes (Apostol 2021) can be used, in principle, to estimate the moment of occurrence of the main shock and its magnitude, although with limitations. The main source of errors arises from the quality of the fit $B(t)$ vs $M(t)$ (Eq. (10)), or, equivalently, the fit of the function $R(\theta)$ given by Eq. (9), or the fit given by

Eqs. (12) and (13). These fits are necessarily of a poor quality, due to the abrupt decrease of the function $M(t)$ near the occurrence time t_{ms} of the main shock (equation (12)), or, equivalently, the abrupt decrease of the parameters $B(M)$ and $R(\tau)$ for small values of the variables M and τ . Another source of errors arises from the background parameters t_0 and r (β), which may affect considerably the exponentials in the formula of the time cutoff τ_0 (Eq. (7)). The procedure described above is based on the assumption that the foreshock magnitudes are ordered in time according to the law given by Eq. (6). However, according to the epidemic-type model, the time-ordered magnitudes may be accompanied by smaller-magnitudes earthquakes, such that the law given by Eq. (6) may exhibit lower-side oscillations, and the slope given by Eq. (11) may exhibit upper-side oscillations. Several subsets of correlated foreshocks may be identified (in accordance with the epidemic-type model), as well as the absence of correlations. In spite of all these limitations, a continuous monitoring of the foreshock seismic activity by means of the procedure described in this paper may give interesting information about a possible mainshock. Also, the decrease of the GR parameter in the correlated foreshock sequences and its increase in aftershock sequences, as identified in the previous works (*e.g.*, Gulia and Wiemer 2019), as well as in the present one, is a valuable piece of information.

Acknowledgements

The authors are indebted to the colleagues in the Institute of Earth's Physics, Magurele-Bucharest, for many enlightening discussions. This work was carried out within the Program Nucleu 2019, funded by Romanian Ministry of Research and Innovation, Research Grant #PN19-08-01-02/2019 and PN #PN19-06-01-01/2019. Data used for the Vrancea region have been extracted from the Romanian Earthquake Catalog, 2018.

REFERENCES

Apostol, B. F. (2006). Model of Seismic Focus and Related Statistical Dis-

tributions of Earthquakes. Phys. Lett. **A357** 462-466,
doi: 10.1016/j.physleta.2006.04.080.

Apostol, B. F. (2019). An inverse problem in seismology: derivation of the seismic source parameters from P and S seismic waves. J. Seismol. **23** 1017-1030.

Apostol, B. F. (2021). Correlations and Bath's law. Results in Geophysical Sciences. **5** 100011.

Apostol, B. F. & Cune, L. C. (2021). Prediction of Vrancea Earthquake of November 30 2021. Seism. Bull. **2**, Internal Report National Institute for Earth's Physics, Magurele.

Bhattacharya, P., Chakrabarti, C. K., Kamal & Samanta, K. D. (2009). Fractal models of earthquake dynamics. Schuster, H. G., ed., *Reviews of Nonlinear Dynamics and Complexity* pp.107-150. NY: Wiley.

Bollettino Sismico Italiano (2002-2012), <http://bolettinosismica.rm.ingv.it>.

Dascher-Cousineau, K., Lay, T., Brodsky, E. E. (2020). Two foreshock sequences post Gulia and Wiemer (2019). Seism. Res. Lett. **91** 2843-2850.

Dascher-Cousineau, K., Lay, T., Brodsky, E. E. (2021). Reply to "Comment on 'Two foreshock sequences post Gulia and Wiemer (2019)' by K. Dascher-Cousineau, T. Lay, and E. E. Brodsky" by L. Gulia and S. Wiemer. Seism. Res. Lett. **92** 3259-3264.

De Santis, A., Cianchini, G., Favali, P., Beranzoli, L., Boschi, E. (2011). The Gutenberg-Richter law and entropy of earthquakes: two case studies in Central Italy. Bull. Sesim. Soc. Am. **101** 1386-1395.

Enescu, B., Struzik, Z., Kiyono, K. (2008). On the recurrence time of earthquakes: insight from Vrancea (Romania) intermediate-depth events. Geophys. J. Int. **172** 395-404.

Frohlich, C. & Davis, S. D. (1993). Teleseismic b values; or much ado about 1.0. J. Geophys. Res. **98** 631-644.

- Gulia, L., Tormann, T., Wiemer, S., Herrmann, M., Seif, S. (2016). Short-term probabilistic earthquake risk assessment considering time-dependent b values. *Geophys. Res. Lett.* **43** 1100-1108.
- Gulia, L., Rinaldi, A. P., Tormann, T., Vannucci, G., Enescu, B., Wiemer, S. (2018). The effect of a mainshock on the size distribution of the aftershocks. *Geophys. Res. Lett.* **45** 13277-13287.
- Gulia, L. & Wiemer, S. (2019). Real-time discrimination of earthquake foreshocks and aftershocks. *Nature* **574** 193-199.
- Gulia, L. & Wiemer, S. (2021). Comment on "Two foreshock sequences post Gulia and Wiemer (2019)" by K. Dascher-Cousineau, T. Lay, and E. E. Brodsky. *Seism. Res. Lett.* **92** 3251-3258.
- Helmstetter, A. & Sornette, D., (2003). Foreshocks explained by cascades of triggered seismicity. *J. Geophys. Res.: Solid Earth* **108**, <https://doi.org/10.1029/2003JB002409>.
- Jones, L. M. (1994). Foreshocks, aftershocks and earthquake probabilities: accounting for the Landers earthquake. *Bull. Seism. Soc. Am.* **84** 892-899.
- Lay, T. & Wallace, T. C. (1995). *Modern Global Seismology*. Academic Press, San Diego, California.
- Lombardi, A. M. (2021). A normalized distance test for co-determining completeness magnitude and b -values of earthquake catalogs. *J Geophys. Res.: Solid Earth* **126** e2020 JB021242 <https://doi.org/10.1029/2020JB021242>.
- Marzocchi, W., Spassiani, I., Stallone, A., Taroni, M. (2020). How to be fooled for significant variations of the b -value. *Geophys. J. Int.* **220** 1845-1856.
- Ogata, Y. (1988). Statistical models for earthquakes occurrences and residual analysis for point processes. *J. Amer. Statist. Assoc.* **83** 9-27.
- Ogata, Y. (1998). Space-time point-process models for earthquakes occurrences. *Ann. Inst. Statist. Math.* **50** 379-402.

- Ogata, Y. & Tsuruoka, H. (2016). Statistical monitoring of aftershock sequences: a case study of the 2015 M_w 7.8 Gorkha, Nepal, earthquake. *Earth, Planets and Space* **68** 44, 10.1186/s40623-016-0410-8.
- Pelletier, J. D. (2000). Spring-block models of seismicity: review and analysis of a structurally heterogeneous model coupled to the viscous asthenosphere, Rundle, J. B., Turcote, D. L. & Klein, W., eds. *Geocomplexity and the Physics of Earthquakes*. vol. 120. NY: Am. Geophys. Union.
- Romanian Earthquake Catalog (2018), <http://www.infp.ro/data/romplus.txt>, 10.7014/SA/RO.
- Saichev, A. & Sornette, D. (2005). Vere-Jones' self-similar branching model. *Phys. Rev.* **E72** 056122.
- Stein, S. & Wysession, M. (2003). *An Introduction to Seismology, Earthquakes, and Earth Structure*, Blackwell, NY.
- Udias, A. (1999). *Principles of Seismology*. Cambridge University Press, NY.

6 Appendix

6.1 Geometric-growth model of energy accumulation in focus

In Apostol (2006) a typical earthquake is considered, with a small focal region localized in the solid crust of the Earth. The dimension of the focal region is so small in comparison to our distance scale, that we may approximate the focal region by a point in an elastic body. The movement of the tectonic plates may lead to energy accumulation in this pointlike focus. The energy accumulation in the focus is governed by the continuity equation (energy

conservation)

$$\frac{\partial E}{\partial t} = -\mathbf{v} \text{grad} E , \quad (14)$$

where E is the energy, t denotes the time and \mathbf{v} is an accumulation velocity. For such a localized focus we may replace the derivatives in equation (14) by ratios of small, finite differences. For instance, we replace $\partial E/\partial x$ by $\Delta E/\Delta x$, for the coordinate x . Moreover, we assume that the energy is zero at the borders of the focus, such that $\Delta E = -E$, where E is the energy in the centre of the focus. Also, we assume a uniform variation of the coordinates of the borders of this small focal region, given by equations of the type $\Delta x = u_x t$, where \mathbf{u} is a small displacement velocity of the medium in the focal region. The energy accumulated in the focus is gathered from the outer region of the focus, as expected. With these assumptions equation (14) becomes

$$\frac{\partial E}{\partial t} = \left(\frac{v_x}{u_x} + \frac{v_y}{u_y} + \frac{v_z}{u_z} \right) \frac{E}{t} . \quad (15)$$

Let us assume an isotropic motion without energy loss; then, the two velocities are equal, $\mathbf{v} = \mathbf{u}$, and the bracket in equation (15) acquires the value 3. In the opposite limit, we assume a one-dimensional motion. In this case the bracket in equation (15) is equal to unity. A similar analysis holds for a two dimensional accumulation process. In general, we may write equation (15) as

$$\frac{\partial E}{\partial t} = \frac{1}{r} \frac{E}{t} , \quad (16)$$

where r is an empirical (statistical) parameter; we expect it to vary approximately in the range $(1/3, 1)$. We note that equation (16) is a non-linear relationship between t and E . The parameter r may give an insight into the geometry of the focal region. This is why we call this model a geometric-growth model of energy accumulation in the focal region.

The integration of equation (16) needs a cutoff (threshold) energy and a cutoff (threshold) time. During a short time t_0 a small energy E_0 is accumulated.

In the next short interval of time this energy may be lost, by a relaxation of the focal region. Consequently, such processes are always present in a focal region, although they may not lead to an energy accumulation in the focus. We call them fundamental processes (or fundamental earthquakes, or E_0 -seismic events). It follows that we must include them in the accumulation process, such that we measure the energy from E_0 and the time from t_0 . The integration of equation (16) leads to the law of energy accumulation in the focus

$$t/t_0 = (E/E_0)^r . \quad (17)$$

The time t in this equation is the time needed for accumulating the energy E , which may be released in an earthquake (the accumulation time). This is the time-energy accumulation equation referred to in the main text.

6.2 Gutenberg-Richter law. Time probability

The well-known Hanks-Kanamori law reads

$$\ln \overline{M} = \text{const} + bM , \quad (18)$$

where \overline{M} is the seismic moment, M is the moment magnitude and $b = 3.45$ ($\frac{3}{2}$ for base 10). In Apostol (2019) the relation $\overline{M} = 2\sqrt{2}E$ has been established, where $\overline{M} = \left(\sum_{ij} M_{ij}^2\right)^{1/2}$ (mean seismic moment), M_{ij} is the tensor of the seismic moment and E is the energy of the earthquake. If we identify the mean seismic moment with \overline{M} in equation (18) we can write

$$\ln E = \text{const} + bM \quad (19)$$

(another *const*), or

$$E/E_0 = e^{bM} , \quad (20)$$

where E_0 is a threshold energy (related to *const*). Making use of equation (17), we get

$$t = t_0 e^{brM} = t_0 e^{\beta M} , \quad (21)$$

where $\beta = br$. From this equation we derive the useful relations $dt = \beta t_0 e^{\beta M} dM$, or $dt = \beta t dM$. If we assume that the earthquakes are distributed according to the well-known Gutenberg-Richter distribution,

$$dP = \beta e^{-\beta M} dM , \quad (22)$$

we get the time distribution

$$dP = \beta \frac{t_0}{t} \frac{1}{\beta t} dt = \frac{t_0}{t^2} dt . \quad (23)$$

This law shows that the probability for an earthquake to occur between t and $t + dt$ is $\frac{t_0}{t^2} dt$; since the accumulation time is t , the earthquake has an energy E and a magnitude M given by the above formulae (equations (20) and (21)). The law given by equation (23) is also derived (Apostol 2021) from the definition of the probability of the fundamental E_0 -seismic events ($dP = -\frac{\partial}{\partial t} \frac{t_0}{t} dt$). We note that this probability assumes independent earthquakes. This time probability is referred to in the main text.

6.3 Correlations. Time-magnitude correlations

If two earthquakes are mutually affected by various conditions, and such an influence is reflected in the above equations, we say that they are correlated to each other. Also, we say that either one earthquake is correlated with the other. Of course, multiple correlations may exist, *i.e.* correlations between three, four, etc earthquakes. We limit ourselves to two-earthquake (pair) correlations. Very likely, correlated earthquakes occur in the same seismic region and in relatively short intervals of time. The physical causes of mutual

influence of two earthquakes are various. In Apostol (2021) three types of earthquake correlations are identified. In one type the neighbouring focal regions may share (exchange, transfer) energy. Since the energy accumulation law is non-linear, this energy sharing affects the occurrence time. We call these correlations time-magnitude correlations. They are a particular type of dynamical correlations. In a second type of correlations two earthquakes may share their accumulation time, which affects their total energy. We call such correlations (purely) dynamical (or temporal) correlations. Both these correlations affect the earthquake statistical distributions; in this respect, they are also statistical correlations. Finally, additional constraints on the statistical variables (*e.g.*, the magnitude of the accompanying seismic event be smaller than the magnitude of the main shock) give rise to purely statistical correlations.

Let an amount of energy E , which may be accumulated in time t , be released by two successive earthquakes with energies $E_{1,2}$, such as $E = E_1 + E_2$ (energy sharing). According to the accumulation law (equation (17))

$$\begin{aligned} t/t_0 &= (E/E_0)^r = (E_1/E_0 + E_2/E_0)^r = \\ &= (E_1/E_0)^r (1 + E_2/E_1)^r , \end{aligned} \tag{24}$$

or

$$t = t_1 \left[1 + e^{b(M_2 - M_1)} \right]^r , \tag{25}$$

where $t_1 = t_0(E_1/E_0)^r$ is the accumulation time of the earthquake with energy E_1 and magnitude M_1 , and M_2 is the magnitude of the earthquake with energy E_2 . From equation (25) we get

$$b(M_2 - M_1) = \ln \left[(1 + \tau/t_1)^{1/r} - 1 \right] , \tag{26}$$

where $t = t_1 + \tau$, τ being the time elapsed from the occurrence of the earthquake 1 until the occurrence of the earthquake 2. If $\tau/t_1 \ll 1$, as in

foreshock-main shock-aftershock sequences, this equation gives, after some simple manipulations,

$$M_2 = \frac{1}{b} \ln \frac{\tau}{\tau_0} , \quad \tau_0 == r t_0 e^{-b(1-r)M_1} . \quad (27)$$

We can see that τ differs from the accumulation time of the earthquake 2 (compare to equation (21)); it is given by parameters which depend on the earthquake 1 (M_1). If the earthquake 1 is viewed as a main shock, then the earthquake 2 is a foreshock or an aftershock. These accompanying earthquakes are correlated to the main shock (and the main shock is correlated to them). Equations (27) are referred to in the main text as the time-magnitude formula (6).

6.4 Correlations. Dynamical correlations

Let us assume that an earthquake occurs in time t_1 and another earthquake follows in time t_2 . The total time is $t = t_1 + t_2$, so these earthquakes share their accumulation time, which affects their total energy. These are (purely) dynamical (temporal) correlations. According to equation (23) (and the definition of the probability), the probability density of such an event is given by

$$-\frac{\partial}{\partial t_2} \frac{t_0}{(t_1 + t_2)^2} = \frac{2t_0}{(t_1 + t_2)^3} \quad (28)$$

(where $t_0 < t_1 < +\infty$, $0 < t_2 < +\infty$). By passing to magnitude distributions ($t_{1,2} = t_0 e^{\beta M_{1,2}}$), we get

$$d^2 P = 4\beta^2 \frac{e^{\beta(M_1 + M_2)}}{(e^{\beta M_1} + e^{\beta M_2})^3} dM_1 dM_2 \quad (29)$$

(where $0 < M_{1,2} < +\infty$, corresponding to $t_0 < t_{1,2} < +\infty$, which introduces a factor 2 in equation (28)). This formula (which is a pair, bivariate statistical distribution) is established in Apostol (2021). If we integrate this

equation with respect to M_2 , we get the distribution of a correlated earthquake (marginal distribution)

$$dP = \beta e^{-\beta M_1} \frac{2}{(1 + e^{-\beta M_1})^2} dM_1 ; \quad (30)$$

if we integrate further this distribution from $M_1 = M$ to $+\infty$, we get the correlated cumulative distribution

$$P(M) = \int_M^\infty dP = e^{-\beta M} \frac{2}{1 + e^{-\beta M}} . \quad (31)$$

equations (30) and (31) are referred to in the main text (equations (1) and (2)).

For $M \gg 1$ the correlated distribution becomes $P(M) \simeq 2e^{-\beta M}$ and $\ln P(M) \simeq \ln 2 - \beta M$, which shows that the slope β of the logarithm of the independent cumulative distribution (Gutenberg-Richter, standard distribution $e^{-\beta M}$) is not changed (for large magnitudes); the correlated distribution is only shifted upwards by $\ln 2$. On the contrary, for small magnitudes ($M \ll 1$) the slope of the correlated distribution becomes $\beta/2$ ($P(M) \simeq 1 - \frac{1}{2}\beta M + \dots$ by a series expansion of equation (31)), instead of the slope β of the Gutenberg-Richter distribution ($e^{-\beta M} \simeq 1 - \beta M + \dots$). The correlations modify the slope of the Gutenberg-Richter standard distribution for small magnitudes. This is the roll-off effect referred to in the main text.